CellPress

Cell Stem Cell
Article

Hypoxia-Inducible Factors Have Distinct and Stage-Specific Roles during Reprogramming of Human Cells to Pluripotency

Julie Mathieu,[1,6,7] Wenyu Zhou,[2,6,7] Yalan Xing,[1,6] Henrik Sperber,[1,3,6] Amy Ferreccio,[1,6] Zsuzsa Agoston,[4,6] Kavitha T. Kuppusamy,[1,6] Randall T. Moon,[4,5,6] and Hannele Ruohola-Baker[1,2,3,6,*]
[1]Department of Biochemistry, University of Washington School of Medicine, Seattle, WA 98109-4714, USA
[2]Department of Biology, University of Washington, Seattle, WA 98109-4714, USA
[3]Department of Chemistry, University of Washington, Seattle, WA 98109-4714, USA
[4]Department of Pharmacology, University of Washington School of Medicine, Seattle, WA 98109-4714, USA
[5]Howard Hughes Medical Institute, University of Washington, Seattle, WA 98109-4714, USA
[6]The Institute for Stem Cell and Regenerative Medicine (ISCRM), University of Washington School of Medicine, Seattle, WA 98109-4714, USA
[7]These authors contributed equally to this work
*Correspondence: hannele@uw.edu
http://dx.doi.org/10.1016/j.stem.2014.02.012

SUMMARY

Pluripotent stem cells have distinct metabolic requirements, and reprogramming cells to pluripotency requires a shift from oxidative to glycolytic metabolism. Here, we show that this shift occurs early during reprogramming of human cells and requires hypoxia-inducible factors (HIFs) in a stage-specific manner. HIF1α and HIF2α are both necessary to initiate this metabolic switch and for the acquisition of pluripotency, and the stabilization of either protein during early phases of reprogramming is sufficient to induce the switch to glycolytic metabolism. In contrast, stabilization of HIF2α during later stages represses reprogramming, partly because of the upregulation of TNF-related apoptosis-inducing ligand (TRAIL). TRAIL inhibits induced pluripotent stem cell (iPSC) generation by repressing apoptotic caspase 3 activity specifically in cells undergoing reprogramming but not human embryonic stem cells (hESCs), and inhibiting TRAIL activity enhances human iPSC generation. These results shed light on the mechanisms underlying the metabolic shifts associated with the acquisition of a pluripotent identity during reprogramming.

INTRODUCTION

In contrast to differentiated cells, human embryonic stem cells (hESCs) rely mainly on glycolysis for their source of energy, regardless of oxygen availability (Folmes et al., 2011; Panopoulos et al., 2012; Prigione and Adjaye, 2010; Varum et al., 2011; Zhang et al., 2011; Zhou et al., 2012). Pluripotent cells share this metabolic particularity with cancer cells (Warburg effect) (Cairns et al., 2011). In both cell types, glycolytic genes are upregulated, mitochondrial activity is reduced, and lactate production is significantly increased (Panopoulos et al., 2012; Prigione et al., 2010; Varum et al., 2011; Yanes et al., 2010). Furthermore, it has recently been proposed that the metabolic properties of stem cells and cancer cells are important for their identity (Greer et al., 2012; Rafalski et al., 2012). However, it is not yet clear how stem cells gain this metabolic signature and how they again activate mitochondrial oxidative phosphorylation pathways during differentiation.

The bioenergetics of pluripotent cells can vary depending on their developmental stage. For example, mouse epiblasts stem cells, which are believed to be at the same primed stage as hESCs, are also highly glycolytic, whereas more naive mouse ESCs are bivalent in their energy production, switching from glycolysis to mitochondrial respiration on demand (Zhou et al., 2012). Human induced pluripotent stem cells (iPSCs) are usually reprogrammed from somatic cells to a primed stage and are very metabolically similar to hESCs (Panopoulos et al., 2012; Suhr et al., 2010; Varum et al., 2011). Therefore, a metabolic switch from oxidative to highly glycolytic needs to take place during iPSC formation. Supporting this idea, the inhibition of glycolysis reduces reprogramming efficiency, whereas stimulation of glycolytic activity enhances iPSC generation (Folmes et al., 2011; Panopoulos et al., 2012; Zhu et al., 2010). How iPSCs establish a Warburg-like metabolic phenotype during the reprogramming process is largely unknown.

The dependency of stem cells on glycolysis to produce ATP could be an adaptation to low-oxygen tensions in vivo, given that hypoxia has appeared as a key feature of the stem cell niche (Mohyeldin et al., 2010; Suda et al., 2011). Furthermore, low oxygen levels are beneficial for embryonic stem cells (hESCs), adult stem cells (Danet et al., 2003; Ezashi et al., 2005; Morrison et al., 2000; Simsek et al., 2010; Studer et al., 2000), and cancer cells (Axelson et al., 2005; Cabarcas et al., 2011; Mathieu et al., 2011; Takubo and Suda, 2012). Cellular adaptation to hypoxic conditions is mainly mediated through the activation of the oxygen-sensitive transcription factors, hypoxia-inducible factors (HIFs). In normoxia, HIF1α and HIF2α undergo prolyl hydroxylation, which leads to specific binding to the ubiquitin E3 ligase Von Hippel-Lindau, polyubiquitination, and proteasomal degradation. However, HIF1α and HIF2α are stabilized in low oxygen levels, dimerize with HIF1β, and control the transcription of

multiple target genes, including genes involved in glucose metabolism (Pouysségur et al., 2006; Semenza, 2003). HIF1α is expressed ubiquitously, whereas HIF2α expression is more tissue restricted, and both factors have essential roles during development (Compernolle et al., 2002; Iyer et al., 1998; Ryan et al., 1998). Increasing evidence suggests that HIFs can activate factors involved in pluripotency and regulate the stem cell phenotype in both normal and cancer cells (Ezashi et al., 2005, Takubo and Suda, 2012, Covello et al., 2006; Mathieu et al., 2011, 2013). In addition, hypoxia enhances the generation of iPSCs (Yoshida et al., 2009). However the mode of function of HIFs in the process is not fully understood. Given that HIF2α has been shown to activate Oct4 and that HIF2α-deficient embryos have severely reduced numbers of primordial germ cells (Covello et al., 2006), it is believed to be the HIF family member that regulates stem cells (Das et al., 2012; Franovic et al., 2009; Heddleston et al., 2009; Li et al., 2009; Mohyeldin et al., 2010). However, recent data indicate that HIF1α can also regulate stem cell properties (Takubo et al., 2010; Wang et al., 2011). Therefore, it is important to dissect whether HIF1α and HIF2α are involved in the acquisition of stem cell fate and, in particular, in the mechanism underlying the hypoxia effect in reprogramming and whether HIFs are responsible for the metabolic shift during reprogramming.

We now show that both HIF2α and HIF1α are essential for the metabolic changes required early for iPSC generation in humans. Furthermore, we show that HIF2α is required at early stages, but is detrimental at later stages, of reprogramming. HIF1α and HIF2α are sufficient to induce the stem-cell-specific metabolic switch. However, prolonged HIF2α stabilization represses reprogramming because of the upregulation of TNF-related apoptosis-inducing ligand (TRAIL). These data reveal a similarity between normal reprogramming and cancer progression; both require early metabolic switch induced by HIF1α and HIF2α, and both are sensitive to the presence of TRAIL.

RESULTS

A Metabolic Switch Occurs Early during the Reprogramming Process

The metabolism of primed PSCs differs from the one observed in naive PSCs or many differentiated cells (Varum et al., 2011; Zhou et al., 2012). Primed stem cells show reduced mitochondrial activity and rely on glycolysis, whereas differentiated cells produce the majority of their ATP by mitochondrial oxidative phosphorylation. We used the reprogramming assay (Park et al., 2008; Takahashi et al., 2007; Yu et al., 2007) to analyze the requirements for the acquisition of the metabolic state of primed PSCs. Human fibroblasts were reprogrammed into an iPSC state with the four reprogramming factors Oct4, Sox2, Lin28, and Nanog (OSLN). To characterize the metabolic profiles of the cells, we measured a metabolic parameter that mainly defines the mitochondrial respiration levels, oxygen consumption rate (OCR) under various conditions and treatments with Seahorse Extracellular Flux Analyzer (Zhou et al., 2012). We treated the cells with mitochondrial ATP synthase inhibitor, oligomycin, and then a proton gradient discharger, carbonyl cyanide 4-(trifluoromethoxy)phenylhydrazone (FCCP), in order to measure the maximal turnover of the electron transport chain uncoupled from ATP synthesis. This analysis revealed the maximal mitochondrial reserve in the presence of glucose (Goldsby and Heytler, 1963; Heytler, 1963). Fibroblasts showed significantly higher levels of maximal respiratory capacity than hESCs and iPSCs (Figure 1A; Figure S1A available online). These results, in line with previous findings (Folmes et al., 2011; Prigione and Adjaye, 2010; Hansson et al., 2012), suggest that a switch from oxidative to glycolytic metabolism occurs during the iPSC reprogramming process. Furthermore, we examined the kinetics of the metabolic switch by analyzing the OCR and extracellular acidification rate of the cells at different time points of the reprogramming process and found that the FCCP response after oligomycin treatment was already significantly reduced at day 8 (D8) in reprogramming fibroblasts in comparison to control fibroblasts (Figures 1B, 1C, and S1B–S1D). These data indicate that the metabolic changes initiate early in the reprogramming process and support the previous gene expression and proteomics analysis in mouse and human reprogramming (Folmes et al., 2011; Prigione and Adjaye, 2010; Hansson et al., 2012).

Reprogramming Process Has Hypoxic Expression Signature

To reveal the key metabolic genes involved in the transition, we analyzed the gene expression profiles of reprogramming cells and observed an increased expression of metabolic genes in early (D12) and late (D30) time points of the entire fibroblast population exposed to reprogramming factors (Figures 1D, S1E, and S1F and Table S1). The majority of the increased metabolic genes during early reprogramming are hypoxia-responsive genes (Figure 1E). We validated the early upregulation in reprogramming process for ALDOC, ENO3, and PKM2 by quantitative PCR (qPCR; Figure 1F). Given that the reprogramming experiments were performed in normoxia, we tested whether performing the process in hypoxic conditions would be beneficial (Figure 2A). Indeed, the reprogramming process is significantly more efficient when performed in hypoxic conditions. In comparison to 20% O_2, both 2% and 5% O_2 promote iPSC colony formation in various cell lines, including IMR90, MRC5, and JM1 (Figures 2A, 2B, and S2A–S2C), confirming that hypoxia is beneficial for iPSC induction (Yoshida et al., 2009). Using western blot analysis, we showed that the two main hypoxia-responsive factors, HIF1α and HIF2α, were stabilized in hypoxic reprogramming process (Figures 2C, S2D, and S2E).

To test whether HIF1α and HIF2α are stabilized in the normoxic (20% O_2) reprogramming process, we analyzed multiple time points in normal reprogramming (Figures 2D and S2F). Both HIF1α and HIF2α proteins were stabilized during normoxic reprogramming (Figures 2C, 2D, and S2F). To test whether HIFs are also transcriptionally active during the reprogramming in normoxic oxygen environment, we introduced an HIF reporter that contains six HIF-minimal binding sites in front of enhanced yellow fluorescent protein (eYFP) (Zhou et al., 2011) into the fibroblasts used for reprogramming assay (HFF1). This sensor has shown to react to hypoxia and both HIF1α and HIF2α activity (Zhou et al., 2011) (Figure S2G). By D7 of reprogramming, the fluorescent signal had increased significantly, suggesting that HIF1α and/or HIF2α are activated during the reprogramming process (Figure 2E). However, when iPSC colonies were formed, the signal was highly reduced, suggesting that the viral construct

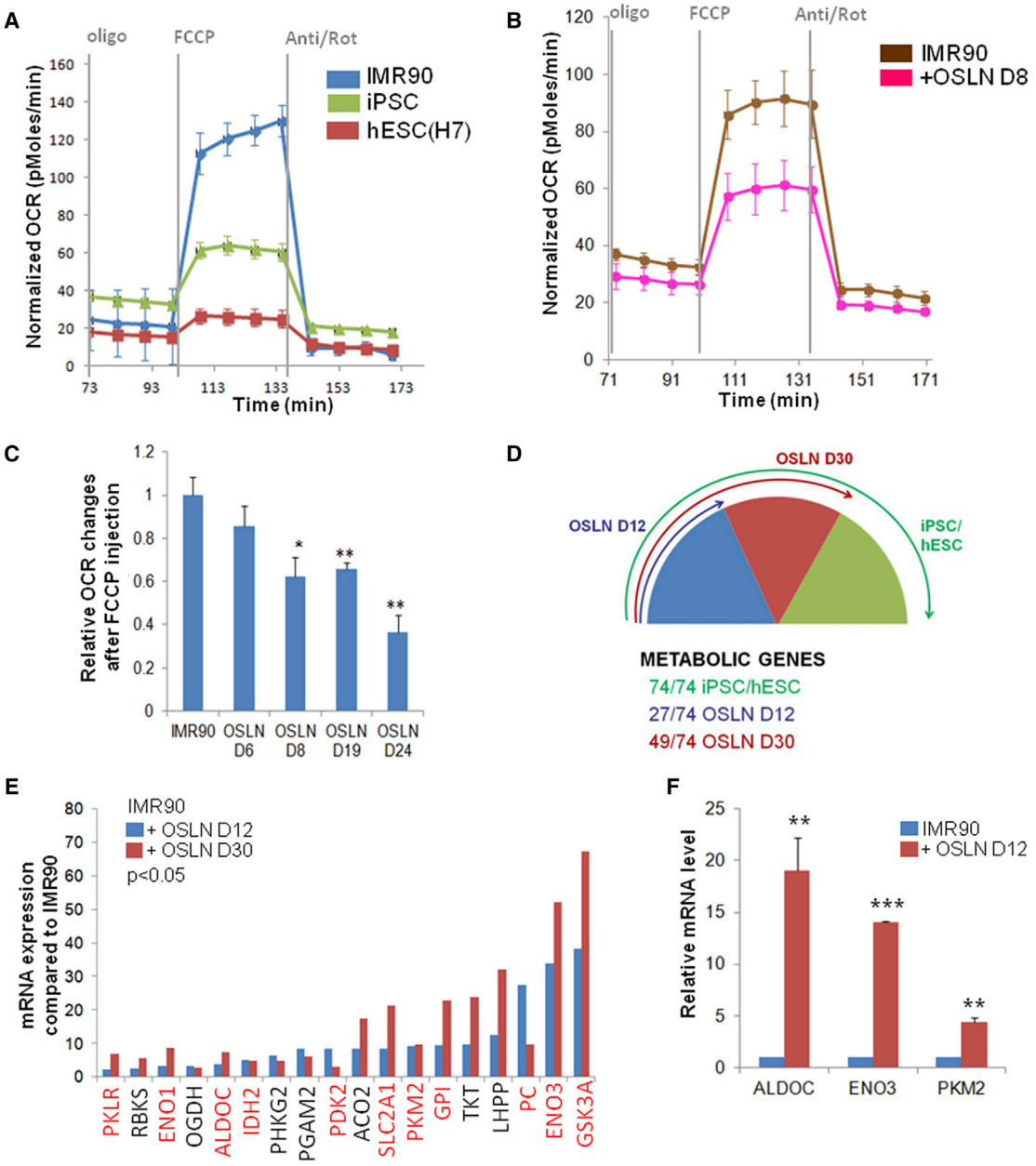

Figure 1. Metabolic Switch Occurs Early in Reprogramming Process

(A) Metabolic profile comparing hESC H7 and iPSCs to fibroblasts (IMR90). A representative trace of OCR changes is shown under mitochondrial stress protocol.

(B) IMR90 OSLN reprogramming cells have reduced OCR change at day 8 (D8) in response to FCCP following oligomycin treatment in comparison to the IMR90 fibroblasts.

(C) Kinetics of changes in oxidative metabolism in the entire IMR90 fibroblast population subjected to OSLN factors over the time course of reprogramming process is shown. Significant change was first observed in D8 reprogramming cells, as shown by relative OCR changes after FCCP injection.

(D) Metabolic gene (Table S1) expression patterns display dynamic changes in early (D12) and late (D30, $p = 0.001$) reprogramming cells in comparison to IMR90 fibroblasts. In comparison to IMR90 fibroblasts, 74 metabolic genes show higher expression level in iPSCs and hESCs. Among those 74 genes, 27 are upregulated in early (D12) reprogramming cells, whereas an additional 22 genes (total of 49) are upregulated in late (D30) reprogramming cells. Arrows indicate the proportion of the 74 upregulated genes in each category.

(E) Microarray expression data are shown for metabolic genes that are upregulated more than 2-fold in early (OSLN D12) and late (OSLN D30) IMR90 reprogramming cells in comparison to the IMR90 fibroblasts. Hypoxia-responsive genes are highlighted in red.

(F) qRT-PCR validates the upregulation of some of these hypoxia-responsive genes in early reprogramming fibroblasts in comparison to control IMR90 fibroblasts. p values were calculated with a Student's t test. *$p < 0.05$; **$p < 0.01$; ***$p < 0.001$. Scale bars show SEM for at least three separate experiments. See also Figure S1.

was inactivated in the stem cell stage, as has been observed previously (Takahashi et al., 2007; Xia et al., 2007; Yu et al., 2007).

HIF2α Is Required for the Metabolic Switch during Early Reprogramming

To test whether HIF1α and/or HIF2α are required for the metabolic switch observed during reprogramming, we used HIF1α and HIF2α small hairpin RNA (shRNA) constructs that resulted in a significant reduction of HIF1α and HIF2α protein levels, respectively (Li et al., 2007) (Figures 2F, 2G, S3A, and S3B). Importantly, when either HIF1α or HIF2α were significantly reduced starting from the initiation of the reprogramming process, at the D8–D10 time point, the total OCR increase after FCCP addition was abnormal. Although HIF1α shRNA effect in the metabolic switch was not statistically significant, HIF2α knockdown (KD) significantly blocked the process (Figures 2H–2K and S3C). At D8, the reprogramming cells with HIF2α KD showed a high OCR increase after FCCP treatment that was comparable to fibroblasts. This starkly contrasts the highly reduced OCR detected in the control reprogramming samples (Figures 2H–2K). Furthermore, at the end of the reprogramming process, the number of iPSC colonies was also significantly reduced when HIF2α was knocked down during the process in both normoxia and hypoxia (Figures 2L and S3D). The iPSC colony formation was also highly reduced when HIF1α was knocked down during the process (Figure 2M). The reduction observed in iPSC induction when HIF1α or HIF2α were knocked down was not due to significantly reduced proliferation rates (Figure S3E). Furthermore, we showed a reduction in the key metabolic hypoxia-responsive genes in the reprogramming cells in which HIF1α or HIF2α was knocked down (Figures 2N and S3F). Later in the reprogramming process, an increase of small iPSC-like colonies was observed in some of the HIF1α KD plates (Figures S3G–S3J). Altogether, these data suggest that both HIF2α and HIF1α are required for the metabolic switch that initiates early during the reprogramming process and that this step is necessary for iPSC colony formation.

Reprogramming Process Requires Controlled HIF2α Activity

Because hypoxia is beneficial for reprogramming and HIF2α and HIF1α are required for the process, we tested whether constitutive stabilization of HIF1α and/or HIF2α would enhance iPSC generation by overexpressing nondegradable forms of HIF1α and HIF2α during reprogramming ($Pro^{402,\ 564}$/Ala mutations and $Pro^{405,531}$/Ala mutations, respectively; Figures 3A and S4A) (Yan et al., 2007). HIF1α overexpression (OE) during reprogramming significantly increased the efficiency of iPSC colony formation in normoxia as well as in hypoxia in IMR90 and MRC5 fibroblast cell lines (Figures 3B–3D). However, surprisingly prolonged stabilization of HIF2α significantly repressed the reprogramming process in these conditions (Figures 3B–3D), even in combination with HIF1α (Figures 3B and 3C). To confirm that the morphologically and alkaline phosphatase (AP)-staining-identified colonies consist of true pluripotent cells, we stained all cells late in reprogramming process with TRA-1-60 and quantified the positive cells by FACS analysis (Figures 3E–3G and S4B–S4F). Importantly, similar to the morphological analysis, TRA-1-60-positive cell number was increased when HIF1α was stabilized but significantly reduced with HIF2α stabilization (Figures 3F and 3G). As expected, TRA-1-60 FACS analysis also validated the loss-of-function data (Figures 3F, 3G, and 2M).

This difference in HIF1α OE and HIF2α OE effect on reprogramming was not caused by differences in cell proliferation rates (Figure S3E). The iPSC colonies derived from HIF1α-expressing or control samples displayed hESC-like morphology, self-renewal capacity, AP activity, and endogenous NANOG and OCT4 mRNA expression (Figures 3H, 3I, and S4G). In addition, their metabolic profile resembled the hESC metabolic profile, as evident in the diminished mitochondrial functional reserves induced by FCCP following oligomycin treatment (Figure 3J). Cells in these iPSC colonies were pluripotent, given that they had the capacity to differentiate into all three germ layers, as indicated by upregulation of mesoderm, endoderm, and ectoderm markers in embryoid body (EB) assays (Figure 3K) (Yu et al., 2007). Despite several attempts, we were not able to maintain the few colonies derived from the HIF2α-overexpressing cells. Altogether, these data show that, although continuous and prolonged OE of HIF1α is beneficial for reprogramming process, prolonged HIF2α activation represses iPSC formation.

HIF2α Function at Different Stages of Reprogramming

We showed that a loss of HIF2α is detrimental for reprogramming (Figures 2L and S3D). Surprisingly, although continuous HIF1α activation is beneficial, continuous activation of HIF2α represses iPSC induction, suggesting that the reprogramming process requires tightly controlled HIF2α activity. To understand the timing of HIF2α function in the process, instead of reducing HIF2α levels from the beginning of reprogramming, we infected the cells with shRNA against HIF2α in the middle of the reprogramming process (D12) and measured the total number of iPSC colonies formed late in the reprogramming process (D33; Figures 3L and 3M). Interestingly, although HIF2α shRNA reduced iPSC colony number significantly when introduced early (D0; Figure 2L), no obvious defect was observed when HIF2α was knocked down in the middle (D12) of the reprogramming process (Figures 3L and 3M). However, when the nondegradable form of HIF2α was overexpressed in the middle of the reprogramming process, the iPSC colony number was significantly reduced (Figures 3L and 3M). These data suggest that HIF2α is required early, but not late, in iPSC induction. Furthermore, HIF2α needs to be downregulated at the latter part of the reprogramming process, given that constitutive activation of HIF2α late in the process causes a significant repression of reprogramming.

HIF1α and HIF2α Overexpression Is Sufficient to Induce Metabolic Changes

To analyze the mechanism of HIF1α and HIF2α action in somatic cells, we expressed constitutively active HIF1α and HIF2α in fibroblasts without the reprogramming factors. First, we validated the HIF1α and HIF2α activity by showing that in MRC5 fibroblast HIF1α and/or HIF2α OE results in the upregulation of HIF target genes carbonic anhydrase 9 and miR-210 (Figures 4A and 4B). To test whether overactivation of HIF1α or HIF2α could affect the metabolism of fibroblasts without the addition of the reprogramming factors, we analyzed the maximum OCR change after FCCP addition in these conditions. Importantly,

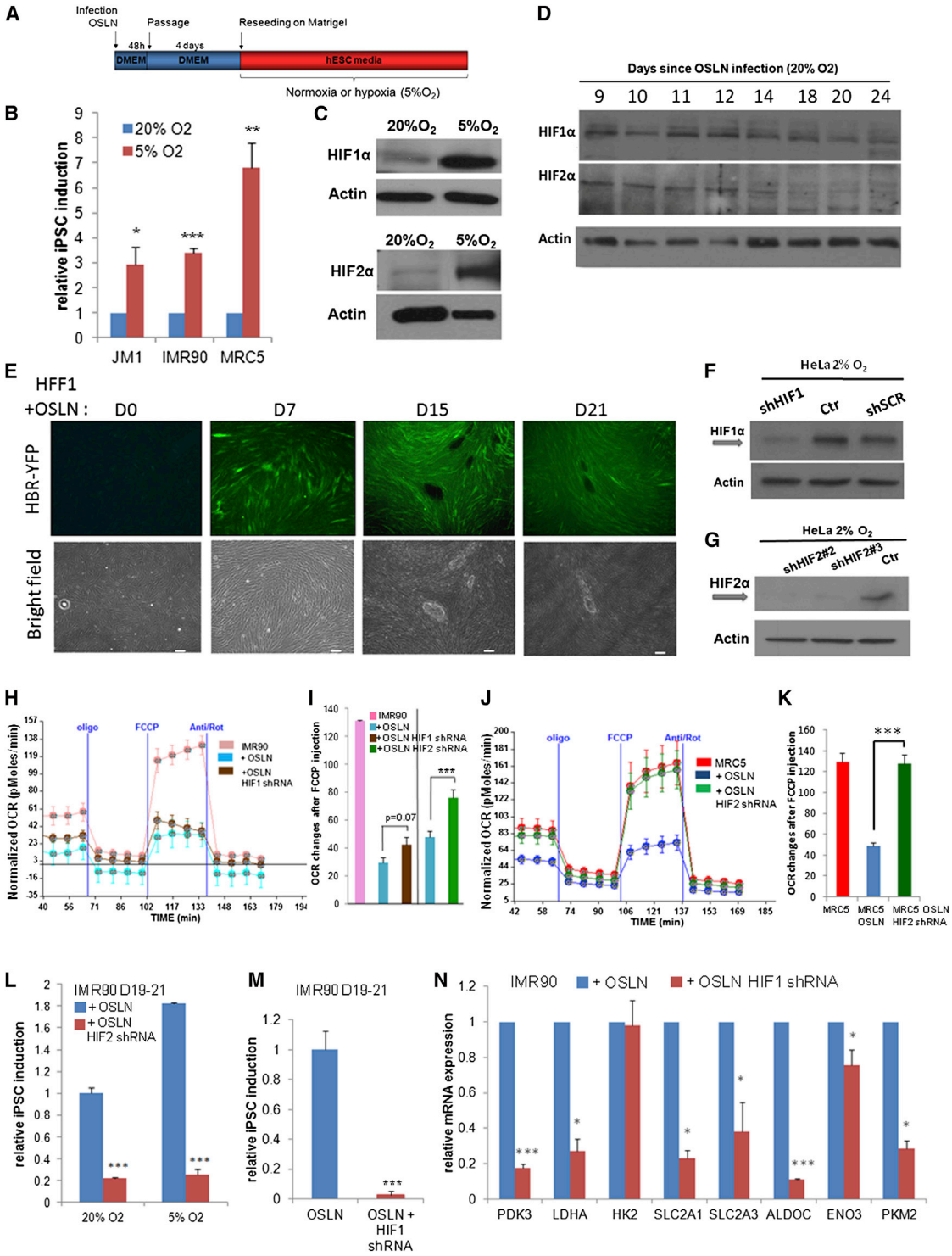

Figure 2. HIFs Are Required for the Metabolic Switch in Early Reprogramming

(A and B) Hypoxia (5% O_2) enhances iPSC formation in three cell lines (JM1, IMR90, and MRC5). Colonies were counted at D21 after OSLN infection.

(C) Comparison of HIF1α and HIF2α protein levels in the reprogramming cells under normoxia (20% O_2 at D9) and hypoxia (5% O_2 at D7).

(D) HIF1α and HIF2α protein stabilization occurs in reprogramming fibroblasts (MRC5) under normoxia, as shown by western blots.

(E) HFF1 cells harboring a YFP hypoxia reporter show an increase of HIF activity during the course of reprogramming. Scale bars represent 200 μm.

(F and G) Western blots validate the KD of HIF1α and HIF2α with shRNA against HIF1α (F) and HIF2α (G), respectively, in HeLa cells.

(H and I) The changes in oxidative metabolism are shown for IMR90, IMR90 infected with OSLN, and IMR90 with OSLN+HIF1α shRNA or OSLN+HIF2α shRNA at D8 of the reprogramming process with a representative trace of OCR under mitochondrial stress protocol (H) and relative OCR changes after FCCP injection (I).

(legend continued on next page)

OE of HIF1α or HIF2α reduced the oxidative metabolism, and this metabolic change was more prominent when both transcription factors were activated simultaneously (Figure 4C). Furthermore, we showed that the observed reduction on mitochondrial activity was not due to the reduction of mitochondrial number by utilizing mitochondrial DNA copy-number assay (Figure 4D). Because no significant change in mitochondrial copy number was found in HIF1α and HIF2α OE cells (Figure 4D), mitochondrial activity regulated by gene expression, rather than mitochondrial number, is critical for the metabolic switch observed in fibroblasts.

Similarly, OCR reduction was accelerated when HIF1α or HIF2α were overexpressed with OSLN during the reprogramming assay (Figure 4E). Therefore, we tested whether HIF1α and/or HIF2α OE would accelerate the increase in expression patterns of metabolic genes observed during reprogramming (Figure 1D). In order to examine the change in gene expression that occurs at various stages of the reprogramming process when HIF2α is OE during OSLN-induced reprogramming, we performed a microarray analysis (Figure S5A). First, we validated the microarray data by showing that stem cell markers were highly enriched in reprogramming cells and that hypoxia target genes were upregulated in HIF2α OE reprogramming cells (Figures S5B and S5C). Our microarray analysis revealed that hypoxia target genes were enriched in HIF2α OE samples in comparison to fibroblasts (Figures S5D and S5E). Furthermore, HIF2α OE and HIF1α OE accelerated the metabolic gene expression during the reprogramming process (Figure S5F). qPCR validation revealed that many of the metabolic genes normally upregulated late in reprogramming process were already upregulated at the D12 time point because of HIF2α and HIF1α overexpression (Figure 4F), suggesting hastened kinetics of the metabolic switch in the reprogramming cells.

Among the metabolic genes upregulated late (D30) during normal reprogramming that were expressed earlier (D12) in HIF1α and HIF2α OE cells was pyruvate dehydrogenase kinase 3 (PDK3; Figures 4F and S5F–S5H). PDK3, an enzyme that blocks the conversion of pyruvate to acetyl-CoA, is significantly enriched in hESCs and hypoxic tumor cells (Mathieu et al., 2011; Stadler et al., 2010). Unlike other PDKs, PDK3 is not inhibited by excess pyruvate and therefore is considered a key regulator for a switch from oxidative to glycolytic metabolism. We studied the kinetics of PDK3 upregulation when HIF1α and/or HIF2α are overexpressed during reprogramming by qRT-PCR. Although, in control, an 8-fold increase in PDK3 expression was observed at D30 of the reprogramming process, HIF1α and HIF2α accelerated this process, given that upregulation of PDK3 was observed at D7 or D12 in reprogrammed MRC5 or IMR90 cells (Figures 4F, 4G, and S5H). Furthermore, we tested whether the inhibition of PDK3 could suppress the HIF1α-induced increase in iPSC formation. Using the chemical inhibitor Radicicol (Kato et al., 2007), we showed that reduction of PDK3 activity reduced the number of iPSC colonies in HIF1α-overexpressing reprogramming cells as well as normal reprogramming cells (Figures 4H and S5I), suggesting an important functional role for PDK3 in HIF1α-induced increase in iPSC induction. However, given that Radicicol did not fully eliminate iPSC induction, additional HIF targets are probably involved in the process.

These data show that HIF1α and HIF2α together are sufficient to induce the metabolic switch in fibroblasts. Similarly, HIF1α and HIF2α stabilization in hypoxic cells is shown to be invariably sequential (Keith et al., 2012; Zhou et al., 2011). These data support the hypothesis that HIF1α and HIF2α have a combinatorial, perhaps sequential, role in the metabolic switch observed in early iPSC induction. However, although HIF1α stabilization is beneficial for the process, HIF2α stabilization late in the process is surprisingly detrimental for iPSC induction.

HIF2α Inhibits Reprogramming through TRAIL

In accordance with the observation that HIF2α is required early, but not late, in reprogramming, we also observed that both MRC5 and IMR90 fibroblasts with HIF2α OE give rise to approximately equal or larger number of precolonies in early time points in comparison to the controls (before D14; Figures 5A, S6A, and S6B), suggesting that HIF2α overexpression is beneficial during the early phase of reprogramming. However, a significant repression in colony formation and PDK3 expression was observed in HIF2α overexpressing samples at later time points (Figures 4G, 4H, 5A, and S6A). Similarly, HIF2α OE initiated in the middle of reprogramming process (D12) dramatically reduced iPSC colony formation (Figure 3M), suggesting that HIF2α OE late during reprogramming is detrimental for iPSC formation. Therefore, we examined the gene expression profiles of HIF2α-overexpressing and control cells at D30 of the reprogramming process in order to identify the key HIF2α target that can repress iPSC formation.

As expected, the expression of stem cell markers was only enriched in the control samples, not HIF2α OE cells, validating the lack of iPSC colonies (Figures 5B, 5C, S6C, and S6D). Importantly, we identified TRAIL as the most upregulated gene with stabilized HIF2α at late stage of reprogramming in comparison to controls (Figures 5D and S6E). This upregulation of TRAIL was not observed early in reprogramming (Figure S6F) and was specific for HIF2α OE, given that no effect in TRAIL expression was observed with stabilized HIF1α (Figure 5E). Furthermore, the significant upregulation of TRAIL was also observed when HIF2α OE was induced late in reprogramming (D12; Figure 5F) and a trend of TRAIL downregulation was observed in HIF2 KD late reprogramming samples (Figure S6G).

To analyze whether TRAIL expression was sufficient to reproduce the repressive function of HIF2α, we administered

(J and K) The changes in oxidative metabolism are shown for MRC5, MRC5 infected with OSLN, and MRC5 with OSLN+HIF2α shRNA at D8 of the reprogramming process with a representative trace of OCR under mitochondrial stress protocol (J) and relative OCR changes after FCCP injection (K). OCR change in MRC5 with OSLN+HIF2α shRNA is significantly different from that in MRC5 infected with OSLN.

(L) shRNA against HIF2α decreases iPSC colony formation in both 20% and 5% O_2 in comparison to the control.

(M) shRNA against HIF1α reduces the number of colonies observed at days 19–21.

(N) Expression of metabolic genes are reduced at D23 in IMR90 with OSLN+HIF1α shRNA in comparison to the control. p values were calculated with a Student's t test. *$p < 0.05$; **$p < 0.01$; ***$p < 0.001$. Scale bars show SEM for at least three separate experiments.

See also Figures S2 and S3.

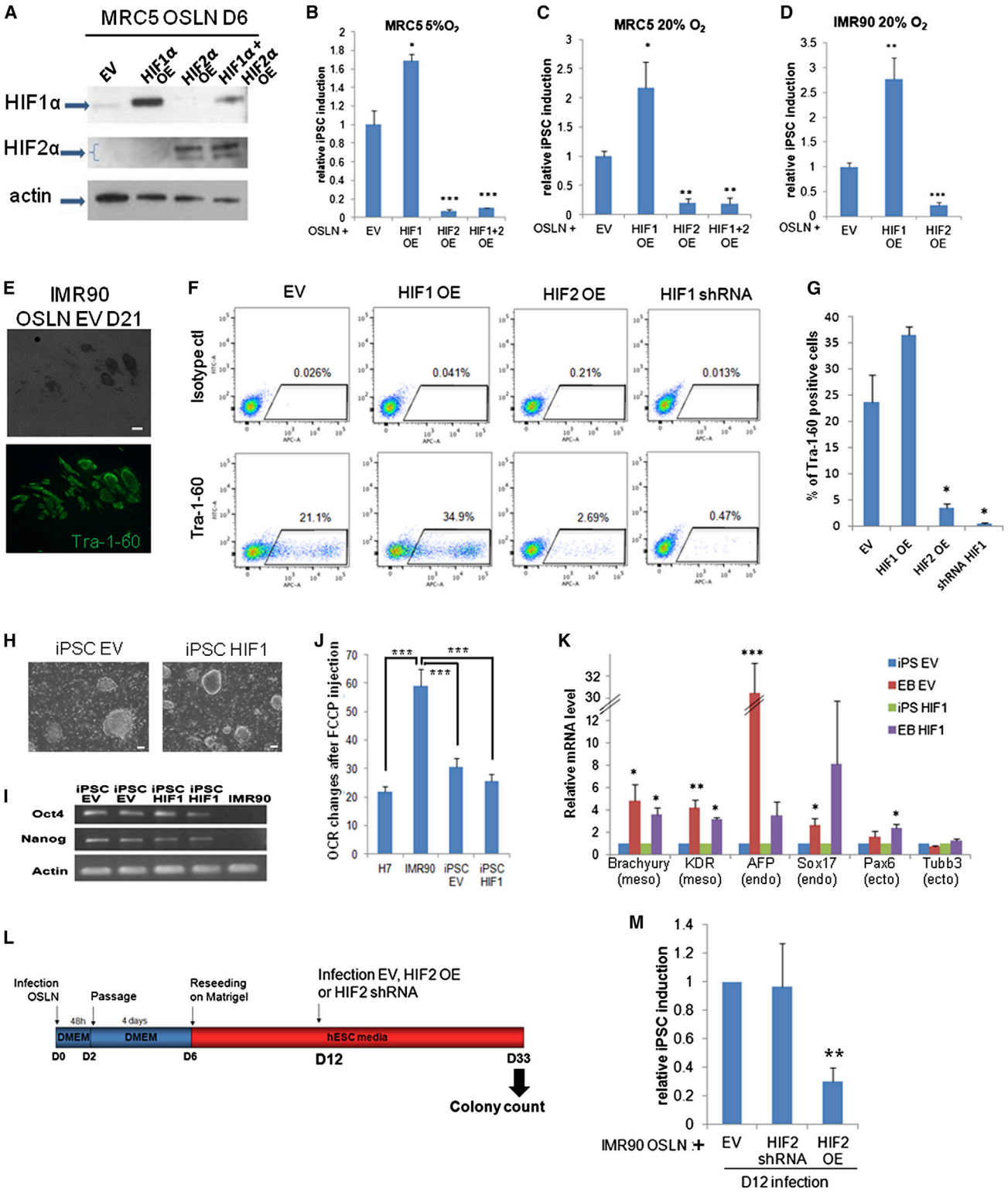

Figure 3. HIF1α and HIF2α Overexpression Have Opposite Effects on Reprogramming

(A) OE of nondegradable HIF1α and HIF2α was confirmed by western blot analysis in MRC5 6 days after OSLN infection.

(B–D) HIF1α OE promotes iPSC colony formation, whereas HIF2α OE inhibits colony formation in 5% (B) and 20% (C) O_2 in MRC5 as well as 20% O_2 in IMR90 (D; n = 7 independent experiments). Colonies were counted at D21 of reprogramming.

(E) Immunofluorescence microscopy shows that colonies counted at 21 days postinfection express the stem cell marker Tra-1-60. The scale bar represents 250 μm.

(legend continued on next page)

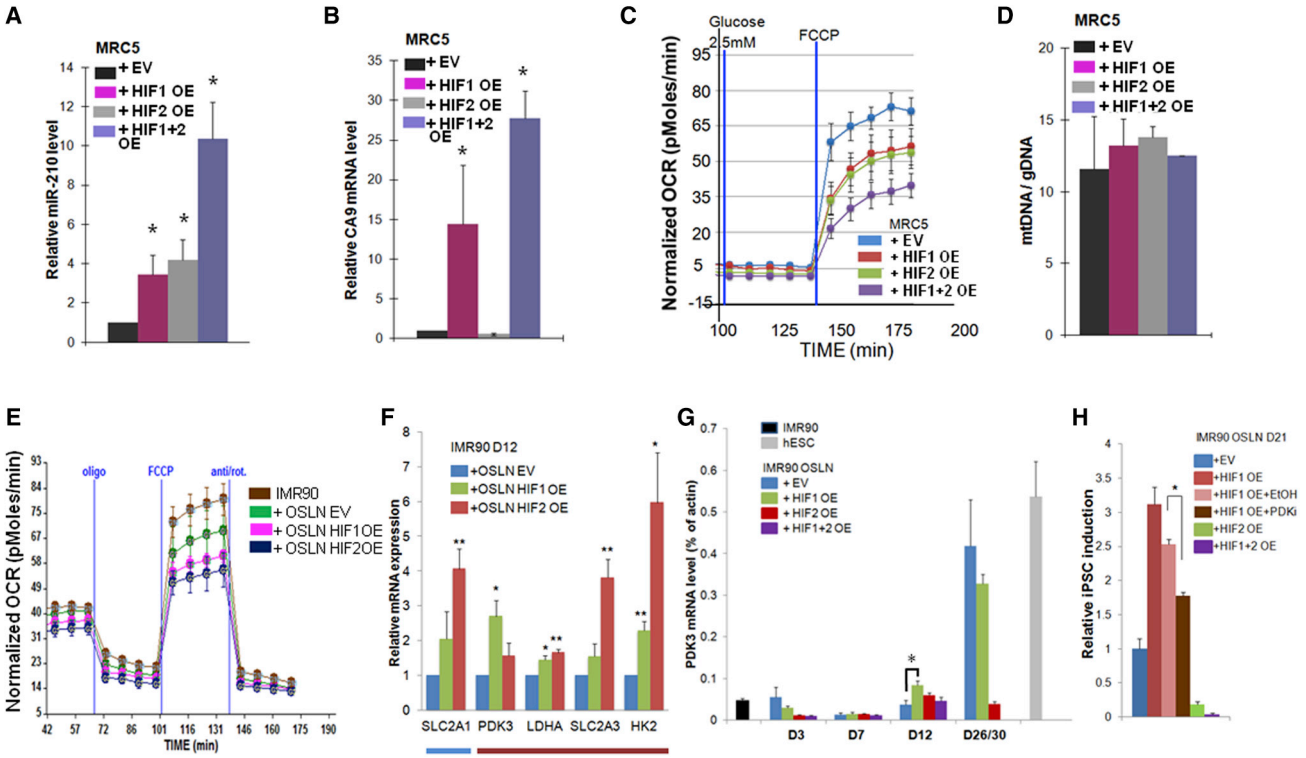

Figure 4. HIF1α and HIF2α Overexpression Are Sufficient to Induce a Metabolic Change

(A–D) In MRC5 fibroblasts infected with HIF1α OE alone, HIF2α OE alone, or HIF1α OE and HIF2α OE together. miR-210 expression was induced both in HIF1α- and HIF2α-overexpressing cells (A), and carbonic anhydrase 9 (CA9) expression was induced only in HIF1α-overexpressing cells (B), confirming the functionality of the overexpressed HIF proteins.

(C) Both HIF1α and HIF2α overexpression in MRC5 fibroblasts without OSLN factors induced glycolytic metabolism similar to hESC H1. Shown are representative Seahorse traces.

(D) Mitochondrial DNA copy number was not changed in HIF1α or HIF2α overexpressing MRC5 fibroblasts.

(E) Both HIF1α and HIF2α overexpression in reprogramming cells (IMR90+OSLN) at D8 resulted in a further decrease in the OCR after FFCP injection.

(F) qPCR validation of the expression level of metabolic genes that were upregulated by HIF1α or HIF2α OE in D12 sample in comparison to the control (blue and red bars indicate the comparative expression in control as illustrated in Figure 1D).

(G) Kinetics of PDK3 mRNA level analyzed by qRT-PCR in IMR90 reprogramming cells is shown as the percentage of actin.

(H) Treatment of PDK3 inhibitor (PDKi) on HIF1α OE cells reduces colony formation in comparison to HIF1α OE cells in the vehicle control (EtOH). p values were calculated with a Student's t test. *$p < 0.05$; **$p < 0.01$. Scale bars show SEM for at least three separate experiments.

See also Figure S5.

TRAIL recombinant protein into the cell-culture media during reprogramming process. Importantly, when 50 or 100 ng/ml of TRAIL was administered to the reprogramming process, fibroblasts continued dividing, but no iPSC colonies were produced (Figures 5G and S6H–S6J), showing that TRAIL mimics HIF2α OE phenotype by repressing the iPSC induction, but not fibroblast viability. Furthermore, we showed that the addition of TRAIL-neutralizing antibody (TRAIL Ab) on HIF2α overexpressing cells was able to counteract HIF2α-repressive function and rescue iPSC formation (Figures 5H

(F) Flow cytometry analysis of Tra-1-60 at D21 after OSLN infection in IMR90.

(G) Quantification of Tra-1-60-positive cells detected by flow cytometry at D21 of reprogramming. Scale bars show SEM for triplicate experiments. Colony count and flow cytometry analysis of those triplicates are presented in Figures S4F and S4D, respectively.

(H–J) iPSC colonies reprogrammed from HIF1α OE IMR90 fibroblasts can self-renew (H), express endogenous Oct4 and Nanog (I), and display a reduced mitochondrial activity similar to hESCs (H7) that is different from the parental fibroblasts (IMR90; J). Scale bars represent 200 μm.

(K) The differentiation abilities of both EV iPSC and HIF1α iPSC derived EBs are demonstrated by qRT-PCR analysis of genes representative of three germ layers. Brachyury and kinase insert domain receptor (KDR) are markers for mesoderm, alpha-fetoprotein (AFP) and Sox17 are markers for endoderm, and Pax6 and Tubb3 are markers for ectoderm.

(L) An experimental scheme is shown to test the requirement and specificity of HIF2α at the later stage of the iPSC reprogramming process.

(M) When infected at D12, HIF2α OE reduces colony formation, whereas HIF2α KD by shRNA shows no significant change in colony formation in comparison to the EV-infected cells. p values were calculated with a Student's t test. *$p < 0.05$; **$p < 0.01$; ***$p < 0.001$. Scale bars show SEM for at least three separate experiments.

See also Figure S4.

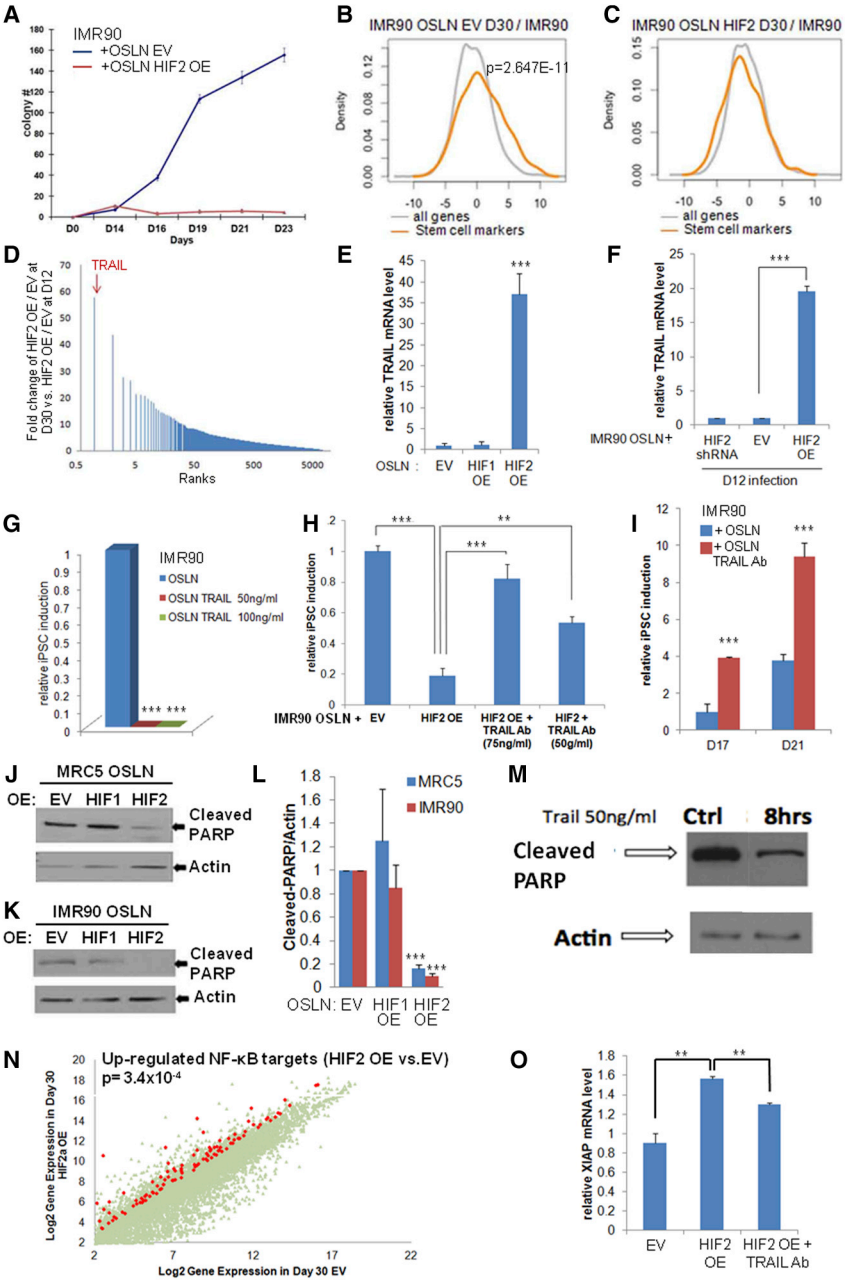

Figure 5. HIF2α Inhibits iPSC Formation through TRAIL Activation

(A) Kinetics of iPSC colony formation in HIF2α OE IMR90 fibroblasts (OSLN+HIF2α), showing an early increase (before D14) but dramatic reduction of iPSC colony formation in late time points in comparison to the control (OSLN+EV).

(B and C) Stem cell markers are significantly upregulated in the control (B), but not HIF2α OE (C), cells during reprogramming.

(D) Microarray analysis reveals that TRAIL is the most upregulated gene at D30 in HIF2α OE reprogramming cells in comparison to normal IMR90 reprogramming cells.

(E) qRT-PCR validation shows the high TRAIL mRNA expression in HIF2α, but not HIF1α, OE reprogramming cells in late time points (D30).

(F) TRAIL mRNA expression analyzed by qRT-PCR increased at late time points (D30) in HIF2α OE cells infected at D12 of the reprogramming process in comparison to OSLN control cells.

(G) Administration of TRAIL during IMR90 reprogramming process (from D7) represses iPSC formation but not fibroblast growth.

(H) Administration of TRAIL antibody on HIF2α-overexpressing cells rescues iPSC formation in IMR90. Colonies were counted at D21.

(I) Administration of TRAIL antibody (75 ng/ml) in the normal reprogramming process (in IMR90) promotes colony formation.

(J–L) In both MRC5 (J) and IMR90 (K) reprogramming cells, HIF2α OE represses PARP cleavage 5-fold (L) in comparison to EV control and HIF1α OE cells (three independent experiments).

(M) Western blots confirm that PARP cleavage is reduced in reprogramming cells treated with 50 ng/ml TRAIL for 8 hr in comparison to the control.

(N) NF-κB target genes are visualized on a scatter plot comparing HIF2α OE at D30 to EV for those that are expressed 4-fold more in HIF2α OE cells.

(O) Quantification of XIAP expression by qRT-PCR assay shows an increased XIAP expression in HIF2α OE reprogramming cells in comparison to the EV at D27. Importantly, such an increase is reduced in HIF2α OE reprogramming cells treated with TRAIL Ab. p values were calculated with a Student's t test. $^{**}p < 0.01$ and $^{***}p < 0.001$. Scale bars show SEM for at least three separate experiments.

See also Figure S6.

and S6K–S6L). These data show that HIF2α exerts its dominant repression at the late stage of reprogramming through TRAIL.

TRAIL Effect in Reprogramming

To test whether TRAIL is normally expressed and has a repressive effect during normal reprogramming, we added TRAIL Ab during normal reprogramming (from D7 on) and counted the iPSC colony number at D17 and D21 in the process. Importantly, the colony number was significantly increased when endogenous TRAIL was sequestered by TRAIL Ab (Figure 5I). The colonies formed were able to undergo self-renewing division and expressed endogenous Oct4 (Figure S6L). These data show that normal reprogramming generates low levels of endogenous TRAIL, which has a repressive property on the reprogramming process, and hence we proceeded to reveal the mechanism of TRAIL action in the process.

TRAIL, by activating a specific set of receptors, can either induce apoptosis through the caspase pathway or display an anti-apoptotic effect, mostly through nuclear factor κB (NF-κB) signaling (Mérino et al., 2007; Walczak et al., 1999). We tested whether HIF2α OE activates the caspase pathway through TRAIL in the reprogramming cells by analyzing the level of cleaved PARP, the cleavage target of active caspase 3. Instead of caspase activation, we observed the repression of caspase, as indicated by the significant reduction of cleaved PARP in

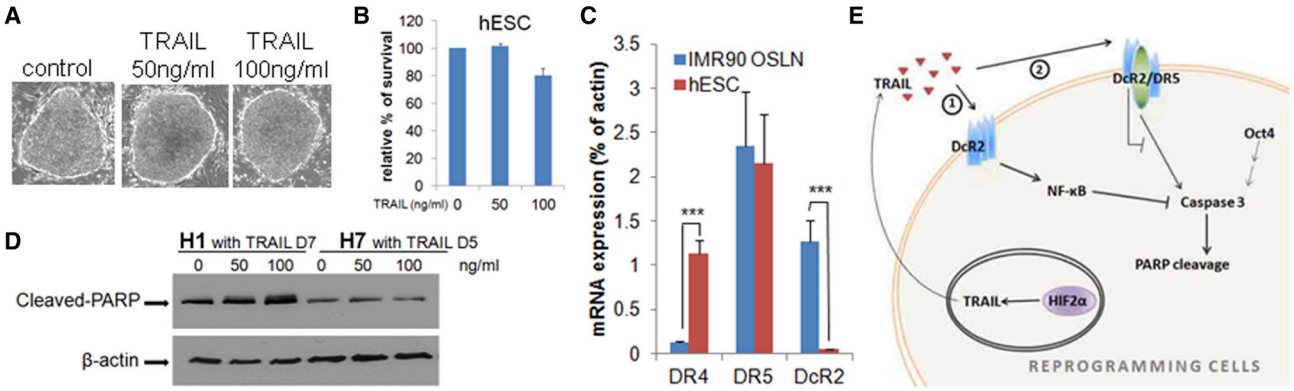

Figure 6. hESCs Bypass TRAIL Effect Due to Low Level of DcR2

(A and B) H1 hESCs can self-renew in the presence of TRAIL in culture. Morphologies (A) and percentage of survival (B) are shown for H1 cells with 50 or 100 ng/ml TRAIL in culture for 7 days in comparison to control H1 cells.

(C) DcR2 mRNA expression is low in hESCs in comparison to reprogramming cells (IMR90 OSLN).

(D) TRAIL administration does not reduce PARP cleavage in H1 or H7.

(E) Models for the repressive action of prolonged HIF2α OE on reprogramming: TRAIL inhibits caspase activity by binding DcR2 and activating NF-κB (1) or binding heteromeric complex of DcR2/DR5 (2). p values were calculated with a Student's t test. ***$p < 0.001$. Scale bars show SEM for at least three separate experiments.

See also Figure S7.

HIF2α, but not HIF1α-overexpressing, reprogramming cells (Figures 5J–5L). Furthermore, we tested whether exogenously added TRAIL protein in the reprogramming system can affect PARP cleavage and found that, 8 hr after TRAIL addition at D17 of iPSC reprogramming, a reduction of PARP was also detected (Figure 5M).

Given that reprogramming cells require active caspases (Li et al., 2010), a reduction of caspase activity could be causal for the lack of iPSC formation in cells constitutively overexpressing HIF2α. Gene expression profiling data further revealed that expression of NF-κB targets, and in particular cFLIP and XIAP, inhibitors of caspase activation, are higher in HIF2α-overexpressing cells than the control (Figures 5N, 5O, and S6M and Table S2), suggesting that TRAIL could induce antiapoptotic activity instead of apoptotic signaling in reprogramming cells. Importantly, TRAIL Ab significantly reduced the upregulation of XIAP observed in HIF2α-overexpressing reprogramming cells (Figure 5O).

hESCs Are Not Responsive to TRAIL

Because reprogramming cells are sensitive to TRAIL, we tested TRAIL effect on pluripotent hESCs and iPSCs and found that, surprisingly, these pluripotent cells can self-renew in the presence of TRAIL (Figures 6A, 6B, and S7A–S7D). Furthermore, we found that this difference in TRAIL responsiveness correlated with differential expression of TRAIL receptors. Although DR4 expression is 10-fold lower in reprogramming cells in comparison to hESCs, decoy receptor 2 (DcR2) expression is significantly higher in fibroblasts (IMR90, 8% of actin; Figure S7E) and reprogramming cells (1.3% of actin) than in hESCs or iPSCs (0.05% of actin; Figures 6C and S7D). Previous data have shown that DcR2, upon binding to TRAIL, can induce NF-κB signaling, which imposes an inhibitory effect on caspase activation (Ehrhardt et al., 2003; Kim et al., 2002). A lower level of DcR2 in hESCs might protect these cells from TRAIL-induced anticaspase signals. Accordingly, in pluripotent cells cultured in the presence of TRAIL for prolonged periods, we found that PARP cleavage is not reduced in comparison to the controls (Figures 6D and S7A–S7C). These results show that TRAIL does not inhibit caspase activity in hESCs or iPSCs.

DISCUSSION

This study shows that reprogramming has distinct stages. Although both HIF1α and HIF2α are required, HIF2α has a stage-specific function in the process. HIF2α is essential in early, but not late, in reprogramming. When stabilized, HIF2α is beneficial in early reprogramming, but prolonged stabilization of HIF2α, in contrast to HIF1α dramatically blocks iPSC formation. We identified the mechanism for prolonged HIF2α repressive action in reprogramming. Through TRAIL, HIF2α inhibits caspase 3 activity, thereby repressing iPSC formation. Unlike reprogramming cells, hESCs can self-renew in the presence of TRAIL in culture. This correlates with the low expression of DcR2 in hESCs.

Human embryonic stem cells are glycolytic (Panopoulos et al., 2012; Prigione et al., 2010; Varum et al., 2011; Zhou et al., 2012), and the reprogramming process undergoes and requires a metabolic switch from oxidative to glycolytic (Armstrong et al., 2010; Panopoulos et al., 2011, 2012; Prigione et al., 2010, 2014; Varum et al., 2011). This metabolic switch precedes the stem cell fate marker expression (Folmes et al., 2011; Zhou et al., 2012). Here, we show, by analyzing the metabolic flux, that the metabolic switch begins early in the reprogramming process. These data are in accordance with recent expression analysis of mouse reprogramming cells and human reprogramming with cMyc as one of the reprogramming factors (Polo et al., 2012; Prigione et al., 2014). Interestingly, both HIF1α and HIF2α enhance and are required for this switch, possibly through separate transcriptional targets (Keith et al., 2012; Loboda et al., 2010). An interesting question is whether the metabolic switch alone is sufficient to

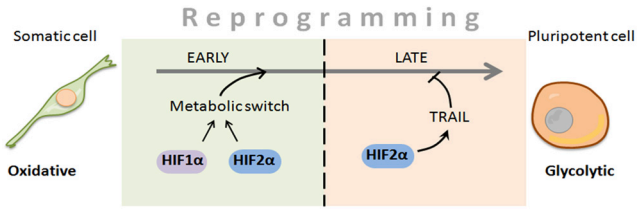

Figure 7. Model of HIF2α Stage-Dependent Role during the Reprogramming Process

When oxidative fibroblasts are reprogrammed into glycolytic pluripotent cells, metabolic switch from oxidative to glycolytic occurs. Our study shows that such a metabolic switch takes place in early stage of the reprogramming process, and HIF1α and HIF2α are essential for this metabolic change. In contrast, constitutive HIF2α stabilization is detrimental for the reprogramming process at the later stage, given that it promotes TRAIL expression, which prevents reprogramming.

initiate the reprogramming process. We showed that prolonged stabilization of HIF1α and HIF2α in fibroblasts is sufficient to induce the metabolic switch from oxidative to highly glycolytic observed in stem cells; however, it was not sufficient to induce pluripotency. This could be due to the repressive effect of HIF2α in iPSC induction through TRAIL. It will be important for future research to test whether switching cell metabolism with more tightly controlled HIFα expression, alone and/or in combination with other factors, could be another avenue for driving somatic reprogramming.

Our findings show that HIF2α is required during the early iPSC reprogramming process to promote the metabolic switch. However, prolonged stabilization of HIF2α represses iPSC formation through TRAIL-induced inhibition of caspase 3 signaling. Previously, it was shown that the activation of apoptotic caspases occurs during the reprogramming process, and their inhibition prevents iPSC generation (Li et al., 2010). Now, we show that HIF2α OE inhibits the caspase 3 activity induced by the reprogramming factors. We also show that HIF2α inhibits iPSC formation through TRAIL. The binding of TRAIL to its cognate receptors DR4 and DR5 activates both apoptotic and nonapoptotic signaling, whereas binding to its decoy receptor 2 (DcR2) only activates antiapoptotic pathways (Degli-Esposti et al., 1997; Sanlioglu et al., 2005). Interestingly, reprogramming cells have a low level of DR4 but a high level of DcR2. In these cells, TRAIL could activate DcR2, and thereby the NF-κB pathway that can repress caspase activity (Ehrhardt et al., 2003; Kim et al., 2002). Furthermore, given that reprogramming cells require an active caspase pathway (Li et al., 2010), TRAIL-dependent caspase inhibition could block iPSC formation (Figure 6E). Our finding that NF-κB targets, and in particular, the antiapoptotic gene XIAP, are upregulated in HIF2α OE reprogramming cells in comparison to controls (Figures 5N and 5O) support this hypothesis. Alternatively, DcR2 could form a heteromeric complex with DR5 and inhibit caspase activation through steric hindrance (Mérino et al., 2006) (Figure 6E). We showed that both fibroblasts and reprogramming cells have higher expression of DcR2 than hESCs, which may be due to low p53 expression in hESCs (Liu et al., 2005). Fibroblasts survive with TRAIL-induced inhibition of the caspase pathway, whereas fibroblasts in the process of becoming iPSCs are sensitive to TRAIL, indicating that similar DcR2 levels in two cell types can lead to different outcomes because of cell-dependent responses to the downstream pathway.

This study presents an example of a significant difference between HIF1α and HIF2α function in the same cellular process. Our results suggest that HIF1α and HIF2α may play nonoverlapping roles in iPSC reprogramming process: HIF1α and HIF2α are essential for the metabolic switch and induction of pluripotency. Additionally, prolonged stabilization of HIF1α increases iPSC induction; however, surprisingly prolonged stabilization of HIF2α significantly represses reprogramming through TRAIL activation (Figure 7). A fine balance exists between the differential roles of the two HIFα factors in early embryonic development, a period when physiological hypoxia is critical for the formation and early differentiation of both germline and somatic stem cells (Dunwoodie, 2009). Our findings in this study provide further evidence on functional difference between HIF1α and HIF2α (Hu et al., 2007; Husa et al., 2010). Reprogramming assays can be used in the future to reveal how structural differences between the two HIFα factors lead to their diverse functional outcomes.

Along with previous studies, this study shows that TRAIL does not induce death in hESCs, cancer stem cells or adult stem cells (Kruyt and Schuringa, 2010). However, TRAIL is detrimental for cancer cells (Mérino et al., 2007; Walczak et al., 1999). Our study now reveals that TRAIL also represses the iPSC reprogramming process. These data suggest a similar mechanism in response to TRAIL in cancer cells and reprogramming cells. In general, the results suggest that cells undergoing reprogramming process may have similar characteristics to the cells undergoing progression toward aggressive tumor cell, allowing us to propose that cancer progression is a slow reprogramming process. First, cancer cells and cells under reprogramming (iPSC induction) both change their metabolism from oxidative to highly glycolytic early during the process. Second, HIFs regulate the switch in both cell types. Third, cancer cells and reprogramming cells are sensitive to TRAIL, whereas cancer stem cells and PSCs are resistant to TRAIL. These similarities between cancer cells and reprogramming cells may allow us to utilize somatic cell reprogramming process in the future as a model for understanding mechanisms and events involved in the cancer progression and to learn from our current knowledge in cancer progression in order to facilitate understanding of the acquisition of pluripotency.

EXPERIMENTAL PROCEDURES

Cell Culture and Reprogramming

hESCs and isolated iPSCs were maintained as previously described (Ware et al., 2006). Reprogramming of human fibroblasts (MRC5, IMR90, and HFF1) was carried out with OSLN lentiviruses (generated from Addgene constructs #21162 and #21163) (Yu et al., 2009). In order to examine hypoxia effect on iPSC formation, cells were cultured under 2% or 5% of O_2 from D7 postinfection. The number of iPSC colonies was defined as the number of AP-, Oct4-GFP-, and/or Tra-1-60-positive colonies. See details in the Supplemental Experimental Procedures.

Overexpression and Inhibition of HIF1α or HIF2α during Reprogramming

Retroviruses expressing nondegradable HIF1α or HIF2α (Addgene constructs #19005 and #19006) (Yan et al., 2007) were infected along with OSLN on D0. An empty vector (EV) construct was used as a control. In order to examine the role of HIF2α in the later stage of the reprogramming process, OSLN

reprogramming cells were infected with HIF2α retrovirus at D12. HIF1α and HIF2α KD were obtained with shRNA constructs (shHIF1α in comparison to shRNA scramble control; Addgene plasmids #22131/shHIF2#2 and #22132/shHIF2#3) (Nemetski and Gardner, 2007; Li et al., 2007). HIF1α and HIF2α OE and KD were validated by western blot analysis.

iPSC Formation with Recombinant TRAIL, TRAIL Ab, or PDK3 Inhibitor Administration

During the iPSC reprogramming process, human TRAIL recombinant protein (R&D Systems; 50 or 100 ng/ml), human TRAIL polyclonal antibody (R&D Systems; 75 or 50 ng/ml), or PDK3 inhibitor Radicicol (Sigma-Aldrich, 36.5 ng/ml) (Kato et al., 2007) were added to OSLN-infected fibroblasts on D7 and every other day along with media change.

Western Blot Analysis, qRT-PCR Analysis, and Mitochondrial DNA Copy-Number Measurement

Standard protocols were used. See details in the Supplemental Experimental Procedures. Primers used in our study are listed in Table S3.

Whole-Genome-Wide Microarray Analysis

Total RNA isolated from IMR90 and MRC5 reprogramming cells infected with HIF2α OE virus or EV control at days 12 and 30 were used in the microarray analysis. RNA qualification, Agilent microarray labeling, hybridization, and scanning were performed in microarray facility at the Institute for Systems Biology. Any intensity-dependent biases were removed in the data with the normalize.qspline function in the affy Bioconductor package.

OCR Measurement with Seahorse Cellular Flux Assays

Mito Stress and Glucose Stress assays were performed on fibroblasts and reprogramming fibroblasts (infected by OSLN) with the Seahorse XF96 Extracellular Flux Analyzer. The OCR values were further normalized to the number of cells and quantified by the Hoechst staining (HO33342; Sigma-Aldrich). See the Supplemental Experimental Procedures for details.

In Vivo Detection of HIF Activity with eYFP Reporting System

In order to test the level of HIF transcriptional activity during reprogramming, fibroblasts were infected with HIF reporter HBR-6U lentivirus (Zhou et al., 2011) before undergoing normal reprogramming assay in normoxia.

Statistical Analysis

Throughout the paper, p values were calculated with Student's t tests. $^{*}p < 0.05$, $^{**}p < 0.01$, $^{***}p < 0.001$. Scale bars show the SEM of at least three separate experiments.

ACCESSION NUMBER

Microarray data have been deposited to the NCBI Gene Expression Omnibus under accession number GSE54898.

SUPPLEMENTAL INFORMATION

Supplemental Information contains Supplemental Experimental Procedures, seven figures, and three tables and can be found with this article online at http://dx.doi.org/10.1016/j.stem.2014.02.012.

ACKNOWLEDGMENTS

We thank Drs. Ware, Hockenbery, and Horwitz and members of the H.R.-B. laboratory for helpful discussions throughout this work. We thank Dr. Stadler for work early in the project. We thank Michael Choi and Timothy Dosey for technical help. We thank Pamela Troisch from Institute for Systems Biology for the microarray gene expression service and Dr. Mecham from Sage Bionetworks for some of the statistical analysis on microarray data. We thank Dr. Gardner for providing the scramble shRNA and shRNA against HIF1α. We also thank members of Tom & Sue Ellison Stem Cell Core for help on iPSC reprogramming procedures and cell cultures. This work was supported by fellowships from the American Heart Association (to J.M., W.Z., and Y.X.), a Tietze Award (to K.T.K.), and grants from the National Institutes of Health (R01GM097372, R01GM083867, and R01GM083867-02S2 to H.R.-B., U01HL100395 to Z.A. and R.T.M., and P01GM081619 to R.T.M. and H.R.-B.).

Received: June 3, 2013
Revised: October 4, 2013
Accepted: February 21, 2014
Published: March 20, 2014

REFERENCES

Armstrong, L., Tilgner, K., Saretzki, G., Atkinson, S.P., Stojkovic, M., Moreno, R., Przyborski, S., and Lako, M. (2010). Human induced pluripotent stem cell lines show stress defense mechanisms and mitochondrial regulation similar to those of human embryonic stem cells. Stem Cells *28*, 661–673.

Axelson, H., Fredlund, E., Ovenberger, M., Landberg, G., and Påhlman, S. (2005). Hypoxia-induced dedifferentiation of tumor cells—a mechanism behind heterogeneity and aggressiveness of solid tumors. Semin. Cell Dev. Biol. *16*, 554–563.

Cabarcas, S.M., Mathews, L.A., and Farrar, W.L. (2011). The cancer stem cell niche—there goes the neighborhood? Int. J. Cancer *129*, 2315–2327.

Cairns, R.A., Harris, I.S., and Mak, T.W. (2011). Regulation of cancer cell metabolism. Nat. Rev. Cancer *11*, 85–95.

Compernolle, V., Brusselmans, K., Acker, T., Hoet, P., Tjwa, M., Beck, H., Plaisance, S., Dor, Y., Keshet, E., Lupu, F., et al. (2002). Loss of HIF-2alpha and inhibition of VEGF impair fetal lung maturation, whereas treatment with VEGF prevents fatal respiratory distress in premature mice. Nat. Med. *8*, 702–710.

Covello, K.L., Kehler, J., Yu, H., Gordan, J.D., Arsham, A.M., Hu, C.J., Labosky, P.A., Simon, M.C., and Keith, B. (2006). HIF-2alpha regulates Oct-4: effects of hypoxia on stem cell function, embryonic development, and tumor growth. Genes Dev. *20*, 557–570.

Danet, G.H., Pan, Y., Luongo, J.L., Bonnet, D.A., and Simon, M.C. (2003). Expansion of human SCID-repopulating cells under hypoxic conditions. J. Clin. Invest. *112*, 126–135.

Das, B., Bayat-Mokhtari, R., Tsui, M., Lotfi, S., Tsuchida, R., Felsher, D.W., and Yeger, H. (2012). HIF-2α suppresses p53 to enhance the stemness and regenerative potential of human embryonic stem cells. Stem Cells *30*, 1685–1695.

Degli-Esposti, M.A., Dougall, W.C., Smolak, P.J., Waugh, J.Y., Smith, C.A., and Goodwin, R.G. (1997). The novel receptor TRAIL-R4 induces NF-kappaB and protects against TRAIL-mediated apoptosis, yet retains an incomplete death domain. Immunity *7*, 813–820.

Dunwoodie, S.L. (2009). The role of hypoxia in development of the Mammalian embryo. Dev. Cell *17*, 755–773.

Ehrhardt, H., Fulda, S., Schmid, I., Hiscott, J., Debatin, K.M., and Jeremias, I. (2003). TRAIL induced survival and proliferation in cancer cells resistant towards TRAIL-induced apoptosis mediated by NF-kappaB. Oncogene *22*, 3842–3852.

Ezashi, T., Das, P., and Roberts, R.M. (2005). Low O2 tensions and the prevention of differentiation of hES cells. Proc. Natl. Acad. Sci. USA *102*, 4783–4788.

Folmes, C.D., Nelson, T.J., Martinez-Fernandez, A., Arrell, D.K., Lindor, J.Z., Dzeja, P.P., Ikeda, Y., Perez-Terzic, C., and Terzic, A. (2011). Somatic oxidative bioenergetics transitions into pluripotency-dependent glycolysis to facilitate nuclear reprogramming. Cell Metab. *14*, 264–271.

Franovic, A., Holterman, C.E., Payette, J., and Lee, S. (2009). Human cancers converge at the HIF-2alpha oncogenic axis. Proc. Natl. Acad. Sci. USA *106*, 21306–21311.

Goldsby, R.A., and Heytler, P.G. (1963). Uncoupling of Oxidative Phosphorylation by Carbonyl Cyanide Phenylhydrazones. Ii. Effects of Carbonyl Cyanide M-Chlorophenylhydrazone on Mitochondrial Respiration. Biochemistry *2*, 1142–1147.

Greer, S.N., Metcalf, J.L., Wang, Y., and Ohh, M. (2012). The updated biology of hypoxia-inducible factor. EMBO J. *31*, 2448–2460.

Hansson, J., Rafiee, M.R., Reiland, S., Polo, J.M., Gehring, J., Okawa, S., Huber, W., Hochedlinger, K., and Krijgsveld, J. (2012). Highly coordinated proteome dynamics during reprogramming of somatic cells to pluripotency. Cell Rep *2*, 1579–1592.

Heddleston, J.M., Li, Z., McLendon, R.E., Hjelmeland, A.B., and Rich, J.N. (2009). The hypoxic microenvironment maintains glioblastoma stem cells and promotes reprogramming towards a cancer stem cell phenotype. Cell Cycle *8*, 3274–3284.

Heytler, P.G. (1963). uncoupling of oxidative phosphorylation by carbonyl cyanide phenylhydrazones. I. Some characteristics of m-Cl-CCP action on mitochondria and chloroplasts. Biochemistry *2*, 357–361.

Hu, C.J., Sataur, A., Wang, L., Chen, H., and Simon, M.C. (2007). The N-terminal transactivation domain confers target gene specificity of hypoxia-inducible factors HIF-1alpha and HIF-2alpha. Mol. Biol. Cell *18*, 4528–4542.

Husa, M., Liu-Bryan, R., and Terkeltaub, R. (2010). Shifting HIFs in osteoarthritis. Nat. Med. *16*, 641–644.

Iyer, N.V., Kotch, L.E., Agani, F., Leung, S.W., Laughner, E., Wenger, R.H., Gassmann, M., Gearhart, J.D., Lawler, A.M., Yu, A.Y., and Semenza, G.L. (1998). Cellular and developmental control of O2 homeostasis by hypoxia-inducible factor 1 alpha. Genes Dev. *12*, 149–162.

Kato, M., Li, J., Chuang, J.L., and Chuang, D.T. (2007). Distinct structural mechanisms for inhibition of pyruvate dehydrogenase kinase isoforms by AZD7545, dichloroacetate, and radicicol. Structure *15*, 992–1004.

Keith, B., Johnson, R.S., and Simon, M.C. (2012). HIF1α and HIF2α: sibling rivalry in hypoxic tumour growth and progression. Nat. Rev. Cancer *12*, 9–22.

Kim, Y.S., Schwabe, R.F., Qian, T., Lemasters, J.J., and Brenner, D.A. (2002). TRAIL-mediated apoptosis requires NF-kappaB inhibition and the mitochondrial permeability transition in human hepatoma cells. Hepatology *36*, 1498–1508.

Kruyt, F.A., and Schuringa, J.J. (2010). Apoptosis and cancer stem cells: Implications for apoptosis targeted therapy. Biochem. Pharmacol. *80*, 423–430.

Li, L., Zhang, L., Zhang, X., Yan, Q., Minamishima, Y.A., Olumi, A.F., Mao, M., Bartz, S., and Kaelin, W.G., Jr. (2007). Hypoxia-inducible factor linked to differential kidney cancer risk seen with type 2A and type 2B VHL mutations. Mol. Cell. Biol. *27*, 5381–5392.

Li, Z., Bao, S., Wu, Q., Wang, H., Eyler, C., Sathornsumetee, S., Shi, Q., Cao, Y., Lathia, J., McLendon, R.E., et al. (2009). Hypoxia-inducible factors regulate tumorigenic capacity of glioma stem cells. Cancer Cell *15*, 501–513.

Li, F., He, Z., Shen, J., Huang, Q., Li, W., Liu, X., He, Y., Wolf, F., and Li, C.Y. (2010). Apoptotic caspases regulate induction of iPSCs from human fibroblasts. Cell Stem Cell *7*, 508–520.

Liu, X., Yue, P., Khuri, F.R., and Sun, S.Y. (2005). Decoy receptor 2 (DcR2) is a p53 target gene and regulates chemosensitivity. Cancer Res. *65*, 9169–9175.

Loboda, A., Jozkowicz, A., and Dulak, J. (2010). HIF-1 and HIF-2 transcription factors—similar but not identical. Mol. Cells *29*, 435–442.

Mathieu, J., Zhang, Z., Zhou, W., Wang, A.J., Heddleston, J.M., Pinna, C.M., Hubaud, A., Stadler, B., Choi, M., Bar, M., et al. (2011). HIF induces human embryonic stem cell markers in cancer cells. Cancer Res. *71*, 4640–4652.

Mathieu, J., Zhang, Z., Nelson, A., Lamba, D.A., Reh, T.A., Ware, C., and Ruohola-Baker, H. (2013). Hypoxia induces re-entry of committed cells into pluripotency. Stem Cells *31*, 1737–1748.

Mérino, D., Lalaoui, N., Morizot, A., Schneider, P., Solary, E., and Micheau, O. (2006). Differential inhibition of TRAIL-mediated DR5-DISC formation by decoy receptors 1 and 2. Mol. Cell. Biol. *26*, 7046–7055.

Mérino, D., Lalaoui, N., Morizot, A., Solary, E., and Micheau, O. (2007). TRAIL in cancer therapy: present and future challenges. Expert Opin. Ther. Targets *11*, 1299–1314.

Mohyeldin, A., Garzón-Muvdi, T., and Quiñones-Hinojosa, A. (2010). Oxygen in stem cell biology: a critical component of the stem cell niche. Cell Stem Cell *7*, 150–161.

Morrison, S.J., Csete, M., Groves, A.K., Melega, W., Wold, B., and Anderson, D.J. (2000). Culture in reduced levels of oxygen promotes clonogenic sympathoadrenal differentiation by isolated neural crest stem cells. J. Neurosci. *20*, 7370–7376.

Nemetski, S.M., and Gardner, L.B. (2007). Hypoxic regulation of Id-1 and activation of the unfolded protein response are aberrant in neuroblastoma. J. Biol. Chem. *282*, 240–248.

Panopoulos, A.D., Ruiz, S., Yi, F., Herrerías, A., Batchelder, E.M., and Izpisua Belmonte, J.C. (2011). Rapid and highly efficient generation of induced pluripotent stem cells from human umbilical vein endothelial cells. PLoS ONE *6*, e19743.

Panopoulos, A.D., Yanes, O., Ruiz, S., Kida, Y.S., Diep, D., Tautenhahn, R., Herrerías, A., Batchelder, E.M., Plongthongkum, N., Lutz, M., et al. (2012). The metabolome of induced pluripotent stem cells reveals metabolic changes occurring in somatic cell reprogramming. Cell Res. *22*, 168–177.

Park, I.H., Zhao, R., West, J.A., Yabuuchi, A., Huo, H., Ince, T.A., Lerou, P.H., Lensch, M.W., and Daley, G.Q. (2008). Reprogramming of human somatic cells to pluripotency with defined factors. Nature *451*, 141–146.

Polo, J.M., Anderssen, E., Walsh, R.M., Schwarz, B.A., Nefzger, C.M., Lim, S.M., Borkent, M., Apostolou, E., Alaei, S., Cloutier, J., et al. (2012). A molecular roadmap of reprogramming somatic cells into iPS cells. Cell *151*, 1617–1632.

Pouysségur, J., Dayan, F., and Mazure, N.M. (2006). Hypoxia signalling in cancer and approaches to enforce tumour regression. Nature *441*, 437–443.

Prigione, A., and Adjaye, J. (2010). Modulation of mitochondrial biogenesis and bioenergetic metabolism upon in vitro and in vivo differentiation of human ES and iPS cells. Int. J. Dev. Biol. *54*, 1729–1741.

Prigione, A., Fauler, B., Lurz, R., Lehrach, H., and Adjaye, J. (2010). The senescence-related mitochondrial/oxidative stress pathway is repressed in human induced pluripotent stem cells. Stem Cells *28*, 721–733.

Prigione, A., Rohwer, N., Hoffmann, S., Mlody, B., Drews, K., Bukowiecki, R., Blümlein, K., Wanker, E.E., Ralser, M., Cramer, T., and Adjaye, J. (2014). HIF1α modulates cell fate reprogramming through early glycolytic shift and upregulation of PDK1-3 and PKM2. Stem Cells *32*, 364–376.

Rafalski, V.A., Mancini, E., and Brunet, A. (2012). Energy metabolism and energy-sensing pathways in mammalian embryonic and adult stem cell fate. J. Cell Sci. *125*, 5597–5608.

Ryan, H.E., Lo, J., and Johnson, R.S. (1998). HIF-1 alpha is required for solid tumor formation and embryonic vascularization. EMBO J. *17*, 3005–3015.

Sanlioglu, A.D., Dirice, E., Aydin, C., Erin, N., Koksoy, S., and Sanlioglu, S. (2005). Surface TRAIL decoy receptor-4 expression is correlated with TRAIL resistance in MCF7 breast cancer cells. BMC Cancer *5*, 54.

Semenza, G.L. (2003). Targeting HIF-1 for cancer therapy. Nat. Rev. Cancer *3*, 721–732.

Simsek, T., Kocabas, F., Zheng, J., Deberardinis, R.J., Mahmoud, A.I., Olson, E.N., Schneider, J.W., Zhang, C.C., and Sadek, H.A. (2010). The distinct metabolic profile of hematopoietic stem cells reflects their location in a hypoxic niche. Cell Stem Cell *7*, 380–390.

Stadler, B., Ivanovska, I., Mehta, K., Song, S., Nelson, A., Tan, Y., Mathieu, J., Darby, C., Blau, C.A., Ware, C., et al. (2010). Characterization of microRNAs involved in embryonic stem cell states. Stem Cells Dev. *19*, 935–950.

Studer, L., Csete, M., Lee, S.H., Kabbani, N., Walikonis, J., Wold, B., and McKay, R. (2000). Enhanced proliferation, survival, and dopaminergic differentiation of CNS precursors in lowered oxygen. J. Neurosci. *20*, 7377–7383.

Suda, T., Takubo, K., and Semenza, G.L. (2011). Metabolic regulation of hematopoietic stem cells in the hypoxic niche. Cell Stem Cell *9*, 298–310.

Suhr, S.T., Chang, E.A., Tjong, J., Alcasid, N., Perkins, G.A., Goissis, M.D., Ellisman, M.H., Perez, G.I., and Cibelli, J.B. (2010). Mitochondrial rejuvenation after induced pluripotency. PLoS ONE *5*, e14095.

Takahashi, K., Tanabe, K., Ohnuki, M., Narita, M., Ichisaka, T., Tomoda, K., and Yamanaka, S. (2007). Induction of pluripotent stem cells from adult human fibroblasts by defined factors. Cell *131*, 861–872.

Takubo, K., and Suda, T. (2012). Roles of the hypoxia response system in hematopoietic and leukemic stem cells. Int. J. Hematol. *95*, 478–483.

Takubo, K., Goda, N., Yamada, W., Iriuchishima, H., Ikeda, E., Kubota, Y., Shima, H., Johnson, R.S., Hirao, A., Suematsu, M., and Suda, T. (2010). Regulation of the HIF-1alpha level is essential for hematopoietic stem cells. Cell Stem Cell *7*, 391–402.

Varum, S., Rodrigues, A.S., Moura, M.B., Momcilovic, O., Easley, C.A., 4th, Ramalho-Santos, J., Van Houten, B., and Schatten, G. (2011). Energy metabolism in human pluripotent stem cells and their differentiated counterparts. PLoS ONE *6*, e20914.

Walczak, H., Miller, R.E., Ariail, K., Gliniak, B., Griffith, T.S., Kubin, M., Chin, W., Jones, J., Woodward, A., Le, T., et al. (1999). Tumoricidal activity of tumor necrosis factor-related apoptosis-inducing ligand in vivo. Nat. Med. *5*, 157–163.

Wang, Y., Liu, Y., Malek, S.N., Zheng, P., and Liu, Y. (2011). Targeting HIF1α eliminates cancer stem cells in hematological malignancies. Cell Stem Cell *8*, 399–411.

Ware, C.B., Nelson, A.M., and Blau, C.A. (2006). A comparison of NIH-approved human ESC lines. Stem Cells *24*, 2677–2684.

Xia, X., Zhang, Y., Zieth, C.R., and Zhang, S.C. (2007). Transgenes delivered by lentiviral vector are suppressed in human embryonic stem cells in a promoter-dependent manner. Stem Cells Dev. *16*, 167–176.

Yan, Q., Bartz, S., Mao, M., Li, L., and Kaelin, W.G., Jr. (2007). The hypoxia-inducible factor 2alpha N-terminal and C-terminal transactivation domains cooperate to promote renal tumorigenesis in vivo. Mol. Cell. Biol. *27*, 2092–2102.

Yanes, O., Clark, J., Wong, D.M., Patti, G.J., Sánchez-Ruiz, A., Benton, H.P., Trauger, S.A., Desponts, C., Ding, S., and Siuzdak, G. (2010). Metabolic oxidation regulates embryonic stem cell differentiation. Nat. Chem. Biol. *6*, 411–417.

Yoshida, Y., Takahashi, K., Okita, K., Ichisaka, T., and Yamanaka, S. (2009). Hypoxia enhances the generation of induced pluripotent stem cells. Cell Stem Cell *5*, 237–241.

Yu, J., Vodyanik, M.A., Smuga-Otto, K., Antosiewicz-Bourget, J., Frane, J.L., Tian, S., Nie, J., Jonsdottir, G.A., Ruotti, V., Stewart, R., et al. (2007). Induced pluripotent stem cell lines derived from human somatic cells. Science *318*, 1917–1920.

Yu, J., Hu, K., Smuga-Otto, K., Tian, S., Stewart, R., Slukvin, I.I., and Thomson, J.A. (2009). Human induced pluripotent stem cells free of vector and transgene sequences. Science *324*, 797–801.

Zhang, J., Khvorostov, I., Hong, J.S., Oktay, Y., Vergnes, L., Nuebel, E., Wahjudi, P.N., Setoguchi, K., Wang, G., Do, A., et al. (2011). UCP2 regulates energy metabolism and differentiation potential of human pluripotent stem cells. EMBO J. *30*, 4860–4873.

Zhou, W., Dosey, T.L., Biechele, T., Moon, R.T., Horwitz, M.S., and Ruohola-Baker, H. (2011). Assessment of hypoxia inducible factor levels in cancer cell lines upon hypoxic induction using a novel reporter construct. PLoS ONE *6*, e27460.

Zhou, W., Choi, M., Margineantu, D., Margaretha, L., Hesson, J., Cavanaugh, C., Blau, C.A., Horwitz, M.S., Hockenbery, D., Ware, C., and Ruohola-Baker, H. (2012). HIF1α induced switch from bivalent to exclusively glycolytic metabolism during ESC-to-EpiSC/hESC transition. EMBO J. *31*, 2103–2116.

Zhu, S., Li, W., Zhou, H., Wei, W., Ambasudhan, R., Lin, T., Kim, J., Zhang, K., and Ding, S. (2010). Reprogramming of human primary somatic cells by OCT4 and chemical compounds. Cell Stem Cell *7*, 651–655.